N-50

canada/yukon economic development agreement

INDIAN AND NORTHERN AFFAIRS CANADA
NORTHERN AFFAIRS: YUKON REGION

Open File 1995-3(T)

MINERALOGICAL ANALYSIS OF ORE SPECIMENS FROM THE RARE EARTH DEPOSIT OF DODGEX LTD.

PART 1 AND PART 2

By

Canada Centre for Mineral and Energy Technology

Canada

Yukon Government

This report is available from:
Exploration and Geological Services Division,
Indian and Northern Affairs Canada,
300 Main Street, Whitehorse, Yukon Y1A 2B5

PROTECTED BUSINESS INFORMATION

MINERALOGICAL ANALYSIS OF ORE SPECIMENS FROM THE RARE EARTH DEPOSIT OF DODGEX LTD.

PART 1:
MINERAL IDENTITIES, COMPOSITIONS AND MODES OF OCCURRENCE

APRIL 1995

MINERAL SCIENCES LABORATORIES
R. Lastra and D. Owens

Work performed for:
J.S. Dodge
Dodgex Ltd.
Whitehorse, Yukon

Job No. 51075

CONFIDENTIAL

MINERAL SCIENCES LABORATORIES
DIVISION REPORT MSL 95-025 (CR)

CANMET

EXECUTIVE SUMMARY

A mineralogical study was conducted on a niobium-bearing rare earth ore from the Lancer deposit in Yukon by the Applied Mineralogy Group as a cost recovery project for Mr. Dodge, President Dodgex Ltd., 14 MacDonald Road, Whitehorse, Yukon. The study was conducted in two parts. One part is to identify the minerals and to determine the compositions and modes of occurrence of the rare earth minerals, and the second part is to determine the relative quantities of the rare earth minerals and to determine their liberation characteristics. The purpose of the study is to provide guidance in processing the ore. This report is on Part 1 of the study (e.g. mineral identification, compositions and occurrence). Two samples labelled "mainvein" and "footwall" were analyzed. It was found that both are mineralogically and chemically similar. They contain, in weight %, 0.9 Zr, 0.4 to 0.7 Nb, 0.1 Y, and 1.36 rare earth elements (0.6 Ce, 0.4 La, 0.2 Nd, small quantities of Pr, Sm, Gd and Dy, and trace amounts of Eu, Tb, Ho, Er, Tm, Yb and Lu).

The Zr occurs as a major constituent of a very fine-grained, poorly crystallized spongy zircon ($ZrSiO_4$). The zircon is present as minute inclusions in silicates, bastnaesite/parisite and columbite.

The Nb occurs as the major constituent of a variety of minerals grouped under the "generic" term niobates, with ferrocolumbite ($Fe^{+2}Nb_2O_6$) and manganocolumbite ($Mn^{+2}Nb_2O_6$) being the main niobium minerals. The niobates are very fine-grained, and occur as inclusions in silicates, carbonates and bastnaesite/parisite.

The main rare earth mineral is monazite ($(Ce,La,Nd,Th)PO_4$), and the secondary rare earth minerals are bastnaesite ($(Ce,La)(CO_3)F$) and parisite ($Ca(Ce,La)_2(CO_3)_3F_2$). The monazite is a rare earth phosphate that contains Ce, La and some Nd. It occurs as discrete grains and as small aggregates up 150 μm in size. The bastnaesite/parisite are also Ce, La and minerals, but they contain some Nd and small amounts of Sm and Gd. They occur as small irregular grains and aggregates, up to 150 μm in size.

A trace of thorium silicate, probably thorite ($ThSiO_4$) was found in the ore, and some of the minor niobates contain minor amounts of uranium.

An image analysis evaluation, which is performed as Part 2 of this study, will provide a sound base for predicting a grind size to liberate the RE minerals (monazite and bastnaesite/parisite), the niobates and zircon.

Keywords: rare earth, monazite, bastnaesite, parisite

CONTENTS

INTRODUCTION

A mineralogical and image analysis study of a rare earth ore from the Lancer deposit in Yukon was undertaken by the Applied Mineralogy Group as a cost recovery project. The deposit is owned by Dodgex Limited, and an MDA grant was contributed by the Yukon Department of Natural Resources for a mineralogical characterization which would provide guidance in processing the ore. A contract was drawn-up between CANMET (CANMET/MSL Project 51075) and Mr. Dodge, President Dodgex Ltd., 14 MacDonald Road, Whitehorse, Yukon on February 3, 1995. Two 100 kilogram samples of the ore were received by CANMET on February 17, 1995 from Mr. Dodge. The samples consisted of rock fragments averaging about 30 cm in size, and were labelled "mainvein" and "footwall".

The mineralogical and image analysis study is performed in two parts. One part is to identify the rare earth minerals and to determine their compositions and modes of occurrence, and the second part is to determine the relative quantities of the rare earth minerals and to determine their liberation characteristic.

This report is on the first part of the study (i.e. identification, compositions and occurrence of the rare-earth bearing minerals).

METHOD OF INVESTIGATION

The rock fragments from the two samples were crushed to -4.7 mm (-4 mesh) and split into 50 Kg sub-samples. One sub-sample of each type was crushed to -1.7 mm (10 mesh). A 2 Kg sample was then split from the "mainvein" and "footwall" sub-samples and ground -295 μm (-48 mesh). Representative portions of the minus 48 mesh samples were removed and pulverized. One portion of the pulverized sample was submitted for chemical analysis to identify and quantify the rare earth elements and another portion submitted for X-ray diffractometer analysis (XRD) to identify the principal rock-forming minerals.

Polished sections were prepared from representative -295 +208 μm (-48+65 mesh) fractions of the two samples. In addition, -147 +45 μm (-100+325 mesh) fractions were separated into sink and float sub-fractions using a heavy liquid with a specific gravity of 3.30. The two sink fractions, in which the heavier ore minerals were concentrated, were also mounted in polished sections.

The polished sections were studied by optical microscopy, scanning electron microscopy (SEM) with qualitative energy dispersive analysis (EDS), and powder X-ray diffraction analysis (XRD). Electron microprobe analyses (EPMA) were conducted on the major rare earth and niobium minerals to confirm their identities and to determine the quantities of rare earth elements and niobium in the minerals. Qualitative EDS spectra of the rare earth minerals are provided to illustrate their complex compositions. Backscattered electron photomicrographs of the significant rare earth minerals observed in the polished sections are included to illustrate their occurrence and associations.

RESULTS

The quantity of ore minerals (rare earth minerals) in the ore as received is extremely sparse. Therefore, characterization of the rare earth minerals is based essentially on mineralogical analyses of the polished sections prepared from the sink fractions.

The results of the chemical and XRD analyses, given in Tables 1 and 2 respectively, suggest that the "mainvein" and "footwall" samples are analogous.

The minerals identified in the ore samples are recorded in Table 3. The order in which they are listed does not necessarily correspond to their order of abundance. The formulae listed are stoichiometric and, because of elemental substitution, may not represent the compositions of the minerals in the ore.

Table 1 - Results of chemical analyses to determine the rare earth contents of the "mainvein" and "footwall" *

	MAINVEIN	FOOTWALL
Element	ppm	ppm
Rb^+	73	32
Sr^+	31	58
Y	1049	1094
Zr^+	8636	9380
Nb^+	4089	6888
Ba^+	317	209
La	3903	3695
Ce	6297	6520
Pr	608	643
Nd	1886	1997
Sm	266	284
Eu	22	23
Gd	209	226
Tb	30	32
Dy	168	186
Ho	30	33
Er	86	93
Tm	12	13
Yb	78	79
Lu	11	10

* Batch No. B95-1323
\+ Not rare earth elements (Levison, 1966).

Table 2 - X-ray diffractometer analyses of the "mainvein" and "footwall"

	MAJOR	MINOR	TRACE
Mainvein	quartz	dolomite	muscovite calcite
Footwall	quartz	albite ankerite	muscovite

Table 3 - Minerals identified in the "mainvein" and "footwall"

MINERAL	FORMULA
RE phosphates	
monazite-(Ce)	$(Ce,La,Nd,Th)PO_4$
RE fluorocarbonates	
bastnaesite-(Ce)	$(Ce,La)(CO_3)F$
parisite-(Ce)	$Ca(Ce,La)_2(CO_3)_3F_2$
Niobates	
ferrocolumbite	$Fe^{+2}Nb_2O_6$
manganocolumbite	$Mn^{+2}Nb_2O_6$
fergusonite-(Y)	$YNbO_4$
niobates-(Ti,Ce,Y)	Undetermined
zircon	$ZrSiO_4$
huttonite/thorite	$ThSiO_4$
Sulphides	
pyrite	FeS_2
sphalerite	$(Zn,Fe)S$
chalcopyrite	$CuFeS_2$
arsenopyrite	$FeAsS$
Oxides	
goethite	$Fe^{+3}O(OH)$
magnetite	Fe_3O_4
Silicates	
quartz	SiO_2
albite	$NaAlSi_3O_8$
pyroxene	$NaFe^{+3}Si_2O_6$
muscovite	$KAl_2(Si_3Al)O_{10}(OH,F)_2$
Carbonates	
ankerite	$Ca(Fe^{+2},Mg,Mn)(CO_3)_2$
dolomite	$CaMg(CO_3)_2$
siderite	$Fe_{+2}CO_3$
calcite	$CaCO_3$
rhodochrosite	$Mn^{+2}CO_3$

OCCURRENCE OF RARE EARTH ELEMENTS AND NIOBIUM

The rare earth elements in the "mainvein" and "footwall" samples are essentially the light lanthanides (La, Ce, Pr, Nd, Pm, Sm, Eu and Gd) and yttrium. Only trace amounts of the heavy lanthanides (Tb, Dy, Ho, Er, Tm, Yb and Lu) were sporadically observed.

The light lanthanides are dominated by cerium (Ce) and lanthanum (La), with small amounts of neodymium (Nd), and trace amounts of samarium (Sm) and gadolinium (Gd). The Ce and La occur largely as constituents of the mineral monazite and less commonly as bastnaesite and parisite. Minor to trace amounts are also present in some ferrocolumbite and manganocolumbite grains.

Neodymium occurs as a constituent of monazite, and small amounts are present in the bastnaesite and parisite. Trace amounts of Nd were also detected in the ferrocolumbite, manganocolumbite and fergusonite-(Y).

Trace quantities of samarium and gadolinium are present in the bastnaesite, parisite and fergusonite-(Y).

No host mineral was found for the significant amount of praseodymium reported by assay (Table 1).

The only indication of the heavy lanthanides was trace amounts of dysprosium detected by qualitative EDS analysis of several columbite grains.

The yttrium content in the ore samples is much less than that of the light lanthanides (Table 1), but its occurrence is as widespread. It is most prevalent as a minor to trace element in zircon and in some of the ferrocolumbite and manganocolumbite grains. Yttrium also constitutes a major element in fergusonite-(Y), yttrocolumbite and a titanium-niobate tentatively identified as aeschynite-(Y).

Niobium occurs in a wide variety of minerals grouped under the generic name of niobates, and is generally a major constituent of the minerals. The niobium minerals include ferrocolumbite, manganocolumbite, yttrocolumbite, fergusonite-(Y), aeschynite-(Y) and pyrochlore. The identification of some of these minerals is tentative, as it is based solely upon qualitative EDS spectra.

GENERAL MINERALOGY OF THE "MAINVEIN" AND "FOOTWALL"

Since very little difference was noted between the "mainvein" and "footwall" samples they are treated and described as samples from one ore.

The RE, niobium and metallic minerals identified in the samples from the Lancer deposit include pyrite, monazite, bastnaesite, zircon, ferrocolumbite, manganocolumbite, yttrocolumbite, fergusonite-(Y), complex niobates, thorium silicate, goethite, magnetite, chalcopyrite, sphalerite and arsenopyrite. The latter four minerals were observed only in trace amounts in the polished sections prepared from the sink products, and are of little or no significance in this ore. They will not be discussed further in this report.

The rock-forming minerals identified in the "mainvein" include major quartz, minor dolomite and traces of muscovite, acmite, calcite, siderite and rhodochrosite (?). The rock-forming minerals in the "footwall" include major quartz, minor ankerite and albite, and trace amounts of muscovite, acmite, siderite and rhodochrosite (?).

DETAILED MINERALOGY OF THE RARE EARTH AND RE-BEARING MINERALS

The rare earth and RE-bearing minerals identified in the ore include monazite, bastnaesite, parisite, zircon, ferrocolumbite, manganocolumbite, niobates and fergusonite-(Y).

MONAZITE

Monazite is a rare-earth phosphate of the light lanthanides. EMPA have shown that Ce is generally the dominant RE element followed by La. Neodymium is present in small but significant amounts (Table 4). A qualitative EDS spectrum which illustrates the composition of monazite is shown in Figure 13.

The monazite occurs essentially as inclusions (grains and small aggregates) in matrixes of silicates and/or carbonates (Fig. 1). These inclusions are between 5 and 120 μm in size. Discrete, crystals with a maximum dimension of 150 μm (Fig. 2) were also observed in the 100 to 325 mesh fraction of the "footwall" sample. Direct association of monazite with the other rare-earth bearing minerals is sporadic; in such instances it is associated with a yttrium-bearing zircon (Fig. 1). Inclusions in monazite are infrequent, but if present, are usually silicates.

BASTŇAESITE/PARISITE

Bastnaesite and parisite are both members of the bastnaesite group of minerals and are fluocarbonates of the light lanthanides. Quantitative EMPA have shown that Ce is the dominant RE element, with major La, minor Nd, and sporadically trace amounts of both Sm and Gd (Table 5). Qualitative EDS spectra which illustrate the compositions of bastnaesite and parisite are shown in Figures 14 and 15 respectively.

Bastnaesite was observed largely as inclusions in silicates, as small aggregates and occasionally as discrete grains (Figs. 2, 3 & 4) in the 100 to 325 mesh fraction. Grain size ranges between 1 and 20 micrometers although aggregates of 150 micrometres were observed. Inclusions are infrequent and usually are formed of zircon, columbite or silicates (Figs. 3 & 4). Parisite was observed only as an intimate intergrowth with bastnaesite (Figs. 5 & 5a).

ZIRCON

The occurrence of zircon is markedly diverse. It occurs almost entirely as inclusions in either silicates, bastnaesite or columbite or, in intergrowths with

Table 4 - Electron microprobe analysis of Monazite*

MAINVEIN

	#1		#2		
Element	wt%	ox. wt%	wt%	ox. wt%	oxide
La	26.0	30.5	24.9	29.2	La_2O_3
Ce	26.0	30.5	27.0	31.6	Ce_2O_3
Nd	3.5	4.1	3.9	4.6	Nd_2O_3
P	12.7	29.1	12.6	28.9	P_2O_5
Totals	68.2	94.2	68.4	94.3	

	#3		#4		
Element	wt%	ox. wt%	wt%	ox. wt%	oxide
La	25.3	29.7	25.3	29.7	La_2O_3
Ce	26.1	30.6	26.1	30.6	Ce_2O_3
Nd	3.7	4.3	3.9	4.5	Nd_2O_3
P	12.9	29.6	12.8	29.3	P_2O_5
Totals	68.0	94.2	68.1	94.1	

* All monazites analyzed for Sm, Gd, Dy, Ca & Y; none were detected.

Table 4 - Electron microprobe analysis of Monazite* (cont'd)

FOOTWALL

	#5		#6		
Element	wt%	ox. wt%	wt%	ox. wt%	oxide
La	22.6	26.5	25.4	29.8	La_2O_3
Ce	26.9	31.5	26.2	30.7	Ce_2O_3
Nd	4.4	5.1	3.7	4.3	Nd_2O_3
P	12.9	29.6	12.8	29.3	P_2O_5
Totals	67.0	92.7	68.2	94.1	

	#7		#8		
Element	wt%	ox. wt%	wt%	ox. wt%	oxide
La	19.4	22.8	23.5	27.6	La_2O_3
Ce	27.6	32.4	26.7	31.3	Ce_2O_3
Nd	6.4	7.5	4.5	5.2	Nd_2O_3
P	12.8	29.3	12.8	29.3	P_2O_5
Totals	66.5	92.0	67.5	93.4	

AVERAGE

Element	wt%	ox. wt%	oxide
La	24.0	28.2	La_2O_3
Ce	26.6	31.1	Ce_2O_3
Nd	4.2	5.0	Nd_2O_3
P	12.8	29.3	P_2O_5
Totals	67.8	93.6	

* All monazites analyzed for Sm, Gd, Dy, Ca & Y; none were detected.

Table 5 - Electron microprobe analysis of Bastnaesite and Parisite*

MAINVEIN

	#1 Bastnaesite		#1 Parisite		
Element	wt%	ox. wt%	wt%	ox. wt%	oxide
La	13.8	16.2	11.2	13.1	La_2O_3
Ce	31.9	37.4	30.4	35.6	Ce_2O_3
Nd	8.8	10.3	8.4	9.8	Nd_2O_3
Sm	0.4	0.5	0.5	0.6	Sm_2O_3
Gd**	0.4	0.5	0.0	0.0	Gd_2O_3
Ca	0.7	1.0	7.1	9.9	CaO
F	9.3	9.3	8.1	8.1	F
Totals	65.3	75.2	65.7	77.1	

	#2 Bastnaesite		#2 Parisite		
Element	wt%	ox. wt%	wt%	ox. wt%	oxide
La	11.6	13.6	12.8	15.0	La_2O_3
Ce	33.0	38.7	28.6	33.5	Ce_2O_3
Nd	11.3	13.2	7.6	8.9	Nd_2O_3
Sm	0.9	1.0	0.5	0.6	Sm_2O_5
Gd**	0.4	0.5	0.2	0.2	Gd_2O_3
Ca	0.2	0.3	6.4	9.0	CaO
F	8.9	8.9	7.3	7.3	F
Totals	66.3	76.2	63.4	74.5	

Table 5 - Electron microprobe analysis of Bastnaesite and Parisite* (cont'd)

	FOOTWALL				
	#3 Bastnaesite		#4 Bastnaesite		
Element	wt%	ox. wt%	wt%	ox. wt%	oxide
La	13.6	16.0	18.2	21.3	La_2O_3
Ce	31.7	37.1	29.3	34.3	Ce_2O_3
Nd	10.0	11.7	7.5	8.7	Nd_2O_3
Sm	0.8	0.9	0.5	0.6	Sm_2O_3
Gd**	0.5	0.6	0.8	0.9	Gd_2O_3
Ca	0.4	0.6	0.3	0.4	CaO
F	9.2	9.2	10.1	10.1	F
Totals	66.2	76.1	66.7	76.3	

* CO_2 not determined
** Values for Gd corrected for enhancement by Ce, La and Nd.

columbite, bastnaesite and silicates (Figs. 1, 3, 7, 8, 9, 10, 11 & 13). It is significant, from the point of view of a RE-bearing mineral, because of its yttrium content. Much of the zircon is spongy, minute and poorly crystallized and therefore, unsuitable for quantitative EMPA. However, sufficient data was obtained by EMPA to confirm that the zircon was yttrium-bearing. The analyses also showed that the yttrium content of the zircon in the "footwall" (mean 3.4 wt% Y; range 1.4 to 6.9 wt% Y) is greater than that of the zircon in the "mainvein" (mean 1.3 wt% Y; range 0.9 to 1.6 wt% Y). A qualitative EDS spectrum which illustrates the composition of zircon is shown in Figure 16.

NIOBATES

A wide variety of minerals grouped under the "generic" term of niobates was found. These minerals are fine-grained, occur intermittently and, are commonly associated with other more dominant rare earth minerals (Figs. 6, 7, and 10). Nearly all are niobium-rich, but titanium occasionally is dominant (mol percent); tantalum is minor and sporadic. Cations in the niobates are diverse and include yttrium, iron, manganese, cerium, thorium, uranium, neodymium, calcium and gadolinium, with one added occurrence of tin and possibly dysprosium. The identities of some niobates were confirmed by EPMA and XRD, whereas the identities of the other niobates were inferred from their EDS spectra. The niobates with confirmed identities are ferrocolumbite and manganocolumbite, and the niobates with inferred identities are yttrocolumbite, fergusonite-(Y), aeschynite-(Y) and pyrochlore.

Columbite: At least three compositionally unique members of the columbite group of minerals are present in the ore. Ferrocolumbite and manganocolumbite were the most frequently encountered niobates, with yttrocolumbite a distant third. Quantitative EMPA (Table 6) in conjunction with qualitative EDS analyses have shown that, in addition to being a major carrier of niobium, the columbite commonly contains small and varying amounts of Ta and Ti, with intermittent small to trace amounts of Y, Ca, Th and U. Yttrocolumbite was appraised solely by qualitative EDS. Qualitative EDS spectra which illustrate the compositions of ferrocolumbite, manganocolumbite and yttrocolumbite are shown in Figures 17, 18 and 19 respectively. Figure 20 shows an

Table 6 - Electron microprobe analysis of columbites/niobates

MAINVEIN

	#1 Ferrocolumbite		#1 Manganocolumbite		
Element	wt%	ox. wt%	wt%	ox. wt%	oxide
Fe	14.0	18.0	4.1	5.3	FeO
Mn	1.7	2.2	11.6	15.0	MnO
Ca	0.0	0.0	0.7	1.0	CaO
Y	0.4	0.5	0.8	1.0	Y_2O_3
Nb	50.6	72.4	51.0	73.0	Nb_2O_5
Ti	2.1	3.5	0.7	1.2	TiO_2
Ta	0.5	0.6	0.5	0.6	Ta_2O_5
Totals	65.3	97.2	69.4	97.1	

	#2 Manganocolumbite		#2 Ferrocolumbite		
Element	wt%	ox. wt%	wt%	ox. wt%	oxide
Fe	5.3	6.8	9.3	12.0	FeO
Mn	10.4	13.4	5.4	7.0	MnO
Ca	0.3	0.4	0.5	0.7	CaO
Y	0.8	1.0	0.4	0.5	Y_2O_3
Nb	50.8	72.7	50.8	72.7	Nb_2O_5
Ti	0.8	1.3	0.5	0.8	TiO_2
Ta	0.7	0.9	0.6	0.7	Ta_2O_5
Totals	69.1	96.5	67.5	94.4	

EDS spectrum of uranium-bearing niobate, Figure 21 of yttrobetafite and Figure 22 of aeschynite.

Like zircon, the occurrence of columbite is diverse and complex. It is present as inclusions in bastnaesite, silicates, silicate/carbonate complexes; it occurs as intergrowths with zircon and bastnaesite; and, it is a host to minute grains of zircon, thorium silicate and other common silicates (Figs. 4, 6, 7, 7a, 8, 9 and 11). The columbite group minerals are very fine-grained and rarely exceed 25 μm in size.

Fergusonite-(Y): A grain of yttrium niobate was found as a small (10 μm) inclusion in carbonate (Fig. 12). Based on its EDS spectra (Fig. 23), which illustrates the composition of the mineral, the grain was identified as either beta-fergusonite or fergusonite-(Y).

OTHER ORE MINERALS

PYRITE

Pyrite occurs as discrete grains and as inclusions in the silicate/carbonate rock. Although some unaltered pyrite was observed in the ore, the vast majority of it has been replaced to some extent by an iron hydroxide (confirmed by XRD as goethite).

THORIUM SILICATE

Minute amounts of a thorium silicate, defined by EDS spectra (Fig. 24) as being either huttonite or thorite was observed in the ore. The mineral occurs as small to minute inclusions in bastnaesite, columbite and zircon (Figs. 4, 11 & 11a).

CONCLUSIONS

The "mainvein" and "footwall" samples from the Lancer deposit in Yukon are mineralogically and chemically similar. They contain, in weight %, 0.9 Zr, 0.4 to 0.7 Nb, 0.1 Y, and 1.36 rare earth elements (0.6 Ce, 0.4 La, 0.2 Nd, small quantities of Pr, Sm, Gd and Dy).

The Zr occurs as a major constituent of a very fine-grained, poorly crystallized spongy zircon ($ZrSiO_4$). The zircon is present as minute inclusions in silicates, bastnaesite/parisite and columbite.

The Nb occurs as the major constituent of a variety of minerals grouped under a "generic" term niobates, with ferrocolumbite ($Fe^{+2}Nb_2O_6$) and manganocolumbite ($Mn^{+2}Nb_2O_6$) being the main niobium minerals. The niobates are very fine-grained, and occur as inclusions in silicates, carbonates and bastnaesite/parisite.

The main rare earth mineral is monazite ($(Ce,La,Nd,Th)PO_4$), and secondary rare earth minerals are bastnaesite ($(Ce,La)(CO_3)F$) and parisite ($Ca(Ce,La)_2(CO_3)_3F_2$). The monazite is a rare earth phosphate that contains Ce, La and some Nd. It occurs as discrete grains and as small aggregates up 150 μm in size. The bastnaesite/parisite are also Ce, La and minerals, but they contain some Nd and small amounts of Sm and Gd. They occur as small irregular grains and aggregates, up to 150 μm in size.

A trace of thorium silicate, probably thorite ($ThSiO_4$) was found in the ore, and some of the minor niobates contain minor amounts of uranium.

It is qualitatively interpreted that grinding to relatively fine grain sizes will be required to liberate enough of the RE minerals (monazite and bastnaesite/parisite) for a reasonable recovery in a moderate grade RE concentrate. The niobates and zircon are finer-grained than the RE minerals and grinding to even finer grain sizes would be required to liberate and recover them.

An image analysis study is needed to determine the grind size for liberating the minerals.

Metallurgical tests will need to be designed on the basis of the image analysis prediction, and will need to be conducted to determine grades and recoveries that can be obtained with existing metallurgical technologies.

ACKNOWLEDGEMENTS

The authors wish to express their appreciation to M. Beaulne for preparation of the concentrates and polished sections of the ore samples; to P. Carrière for the X-ray diffractometer analyses of the ore samples and X-ray powder diffraction analyses of selected minerals; and to personnel in the Chemical assay laboratory for the assays.

REFERENCE

Levison, A.A., (1966) Amer. Min. Vol. 51, 152.

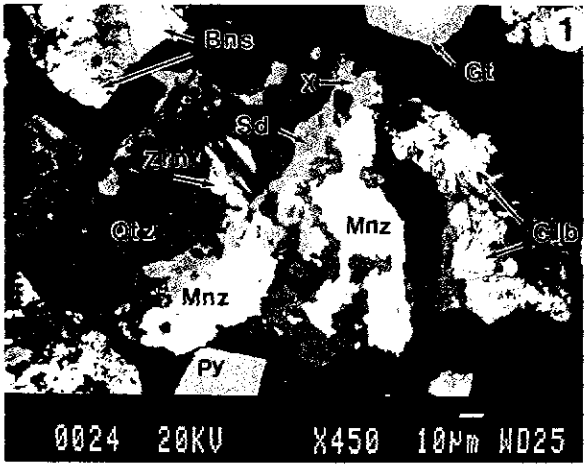

Fig. 1 Backscattered electron (BE) photomicrograph of the polished section (p.s.) prepared from the sink product of the "footwall" showing monazite (Mnz), zircon (Zrn), siderite (Sd), and an unidentified silicate (X) in quartz (Qtz). Bastnaesite (Bns) and manganocolumbite (Clb) are also shown as inclusions in quartz. Pyrite grains (Py), one rimmed by goethite (Gt) are also present in the field.

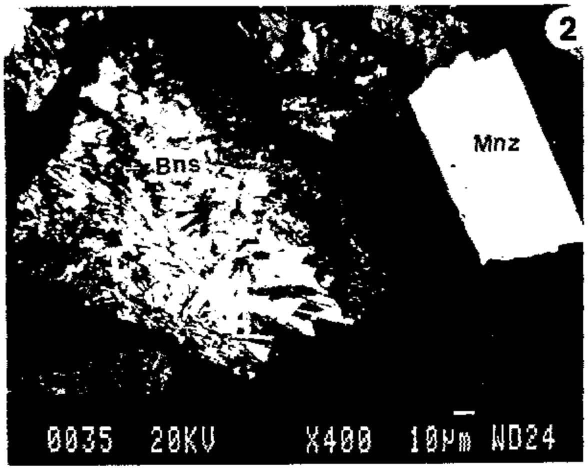

Fig. 2 BE photomicrograph of the p.s. prepared from the sink product of the "footwall" showing a discrete grain of monazite (mnz) and numerous grains of bastnaesite (Bns) in a matrix of albite and ankerite (dark grey).

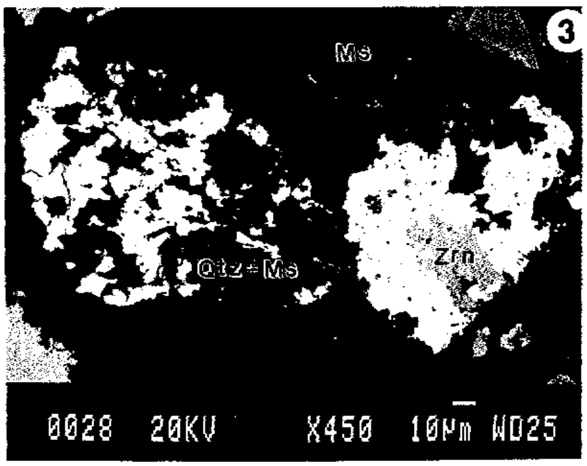

Fig. 3 BE photomicrograph of the p.s. prepared from the sink product of the "footwall" showing bastnaesite disseminated in a silicate matrix of quartz and muscovite (Qtz+Ms) and bastnaesite enclosing zircon (Zrn). Discrete muscovite (Ms) is also visible.

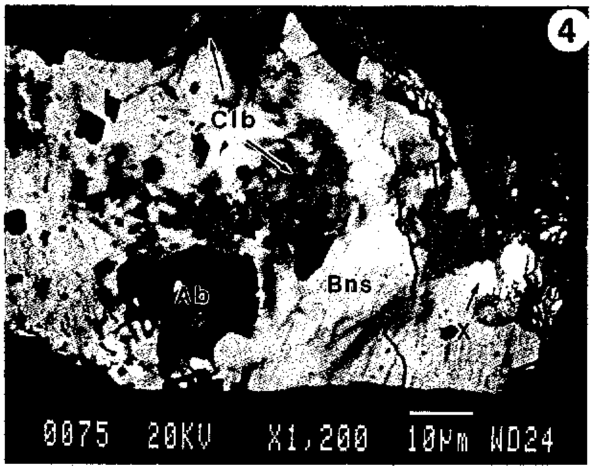

Fig. 4 BE photomicrograph of the p.s. prepared from the sink product of the "footwall" showing ferrocolumbite (Clb), thorium silicate (X) and albite (Ab) locked in bastnaesite (Bns).

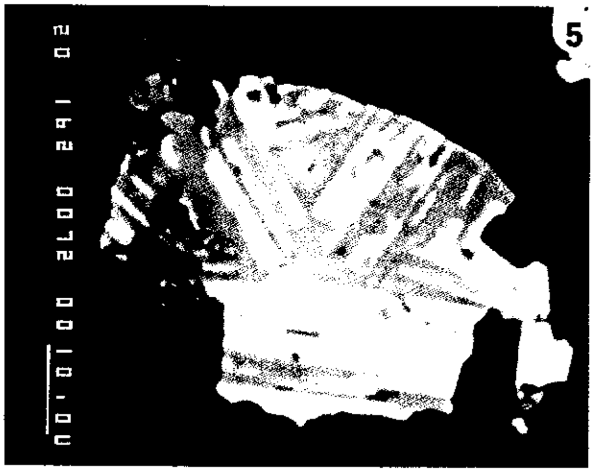

Fig. 5 BE photomicrograph of the p.s. prepared from the sink product of the main-vein showing an intergrowth of bastnaesite (white) and parisite (grey).

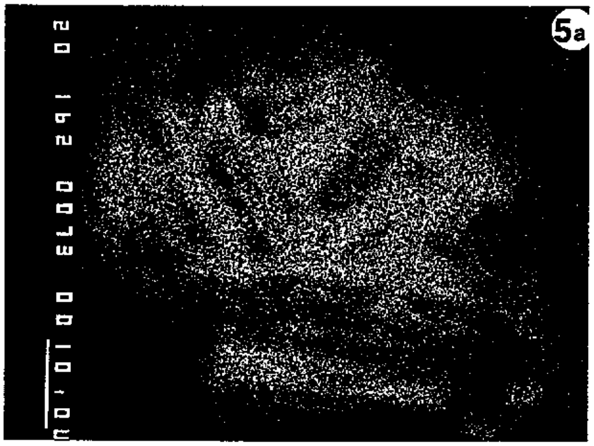

Fig. 5a X-ray photomicrograph for CaKa of the area shown in Fig. 5. The concentrated white dots delineate the calcium-bearing parisite from the bastnaesite.

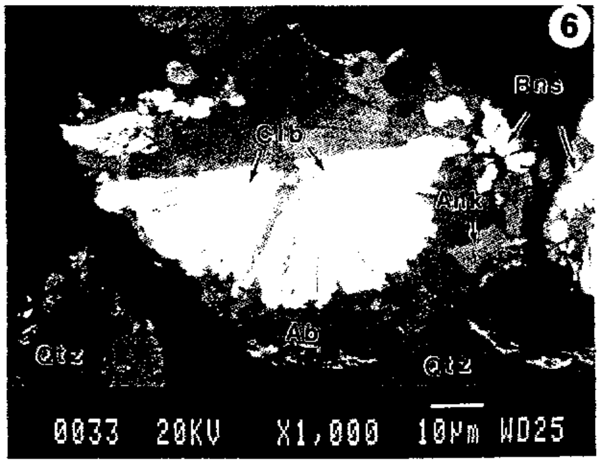

Fig. 6 BE photomicrograph of the p.s. prepared from the sink product of the "footwall" showing a fan of manganocolumbite (Clb) and small grains of bastnaesite (Bns) enclosed in combined quartz (Qtz), albite (Ab) and ankerite (Ank).

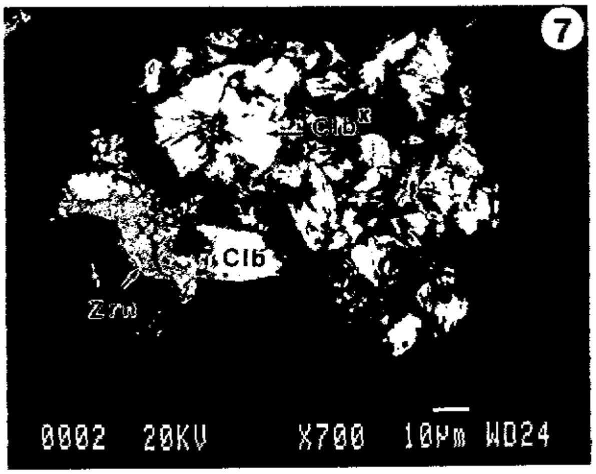

Fig. 7 BE photomicrograph of the p.s. prepared from the sink product of the main-vein showing zircon (Zrn), ferrocolumbite (Clb) and a mixture of ferro-columbite and aeschynite-(Y) (Clb^x) in ankerite (black).

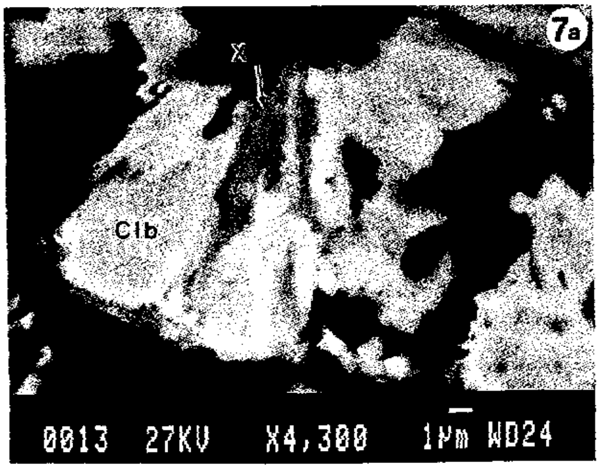

Fig. 7a BE photomicrograph of the area designated Clb^x in Fig. 7 taken at a higher magnification. The dark mineral (X) penetrating and coating the ferro-columbite (Clb) is what has been tentatively identified as aeschynite. The ferrocolumbite exhibits some faint compositional zoning.

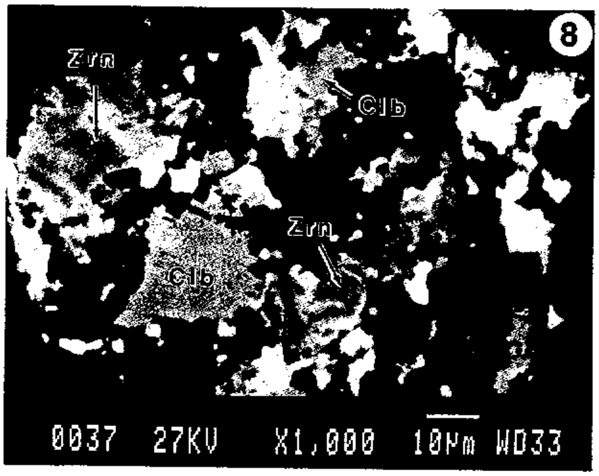

Fig. 8 BE photomicrograph of the p.s. prepared from the sink product of the "footwall" showing combined grains of bastnaesite (white), manganocolumbite (Clb) and zircon (Zrn) in quartz (black).

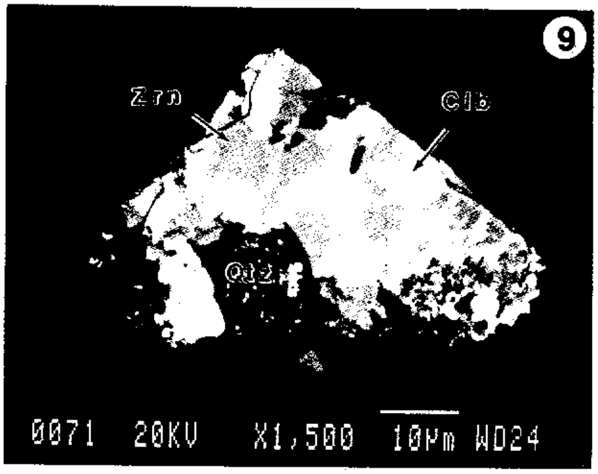

Fig. 9 BE photomicrograph of the p.s. prepared from the sink product of the "footwall" showing yttrocolumbite (Clb) combined with quartz (Qtz) and enclosing minute inclusions of zircon (Zrn).

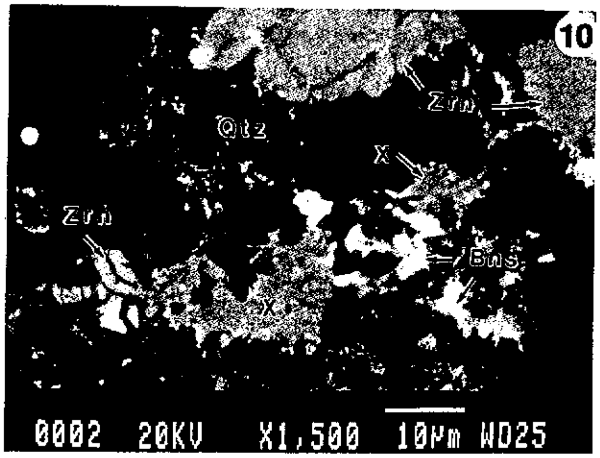

Fig. 10 BE photomicrograph of the p.s. prepared from the -48+65 mesh fraction of the "footwall" sample showing zircon (Zrn), minute bastnaesite (Bns) and a mineral (X) tentatively identified as aeschynite-(Y) as inclusions in quartz (Qtz).

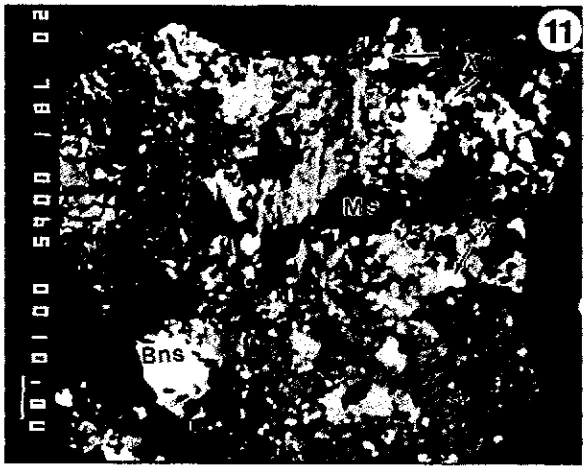

Fig. 11 BE photomicrograph of the p.s. prepared from the sink product of the main-vein showing an intimate intergrowth of fine-grained zircon (dark grey) and ferrocolumbite (light grey) in muscovite (Ms). A number of minute grains of thorium silicate (X) and a larger bastnaesite grain are locked in the complex.

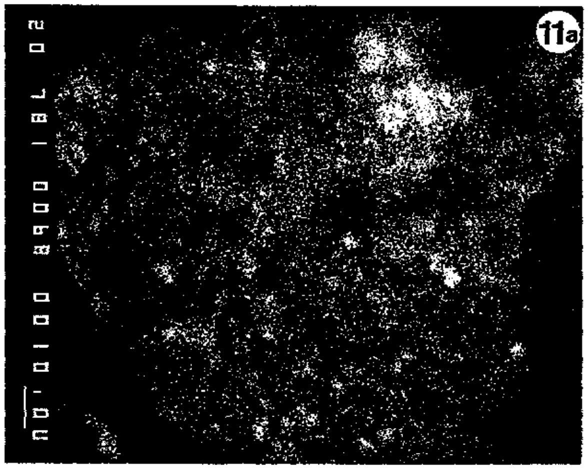

Fig. 11a X-ray photomicrograph for ThLa of the area shown in Fig. 11. The concentrated white dots delineate the inclusions of thorium silicate. The dispersed pattern of dots show that some, but not all of the ferrocolumbite contains minor amounts of thorium.

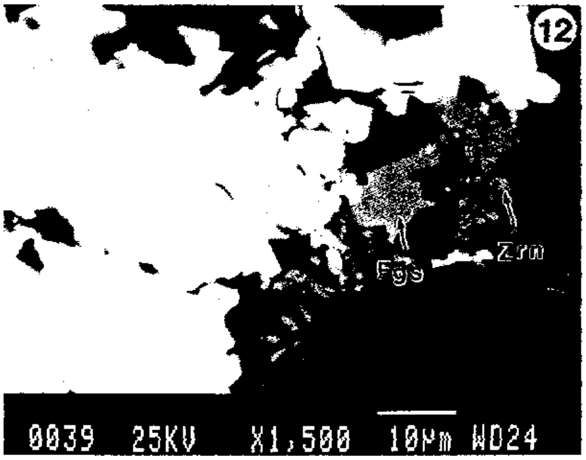

Fig. 12 BE photomicrograph of the p.s. prepared from the sink product of the main-vein showing a small grain of fergusonite-(Y) (Fgs) with zircon (Zrn) and bastnaesite (white) in carbonate (black).

Fig. 13

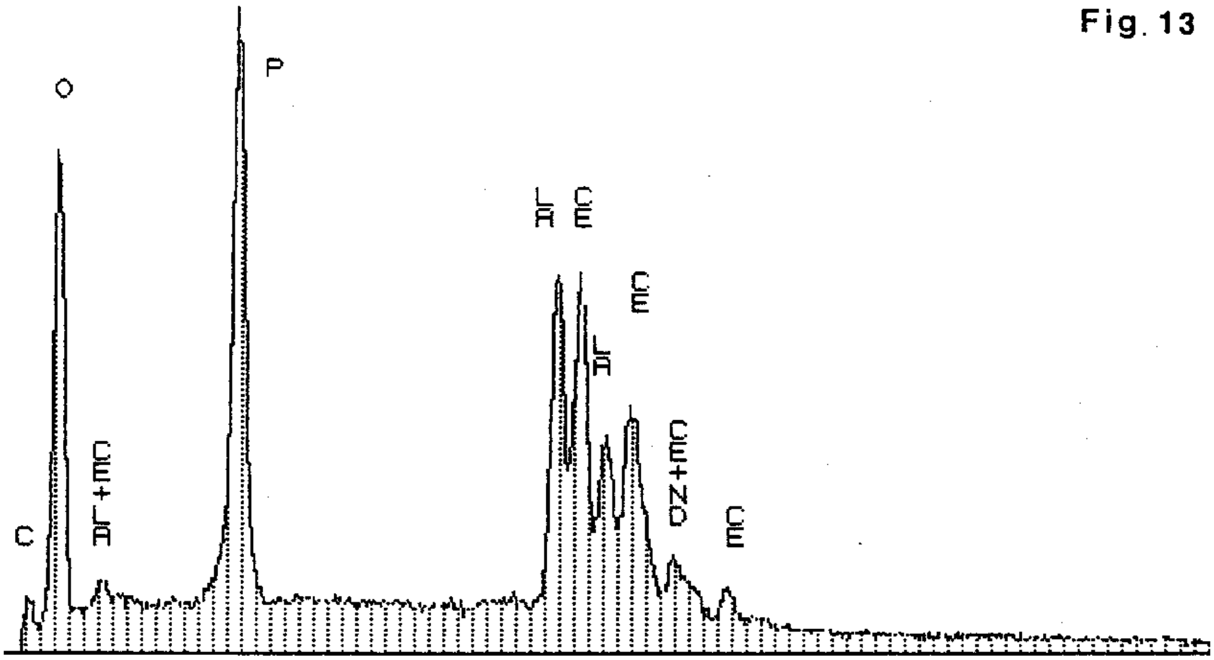

Fig. 14

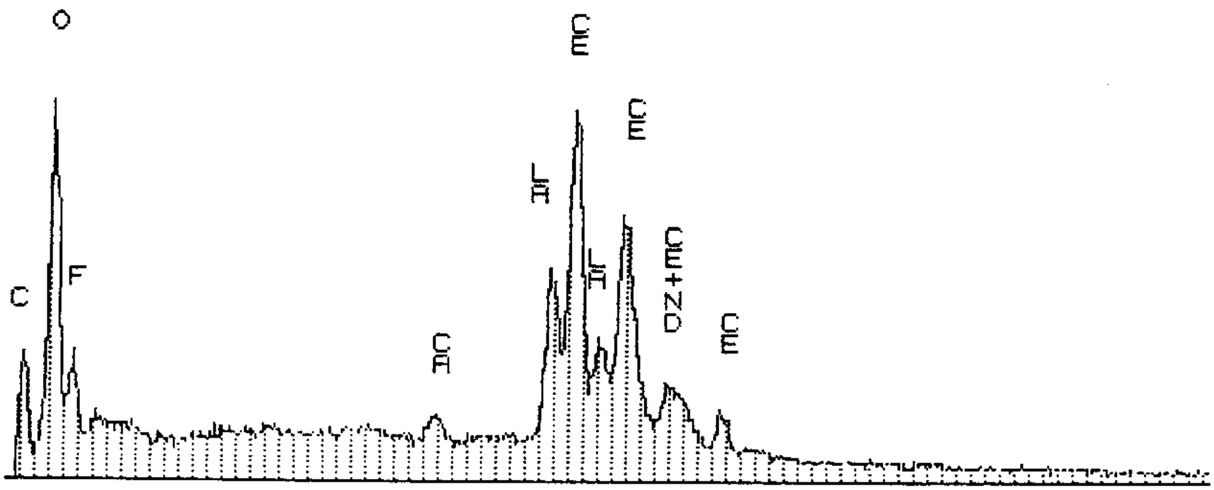

Fig. 13 EDS spectra of monazite.

Fig. 14 EDS spectra of bastnaesite.

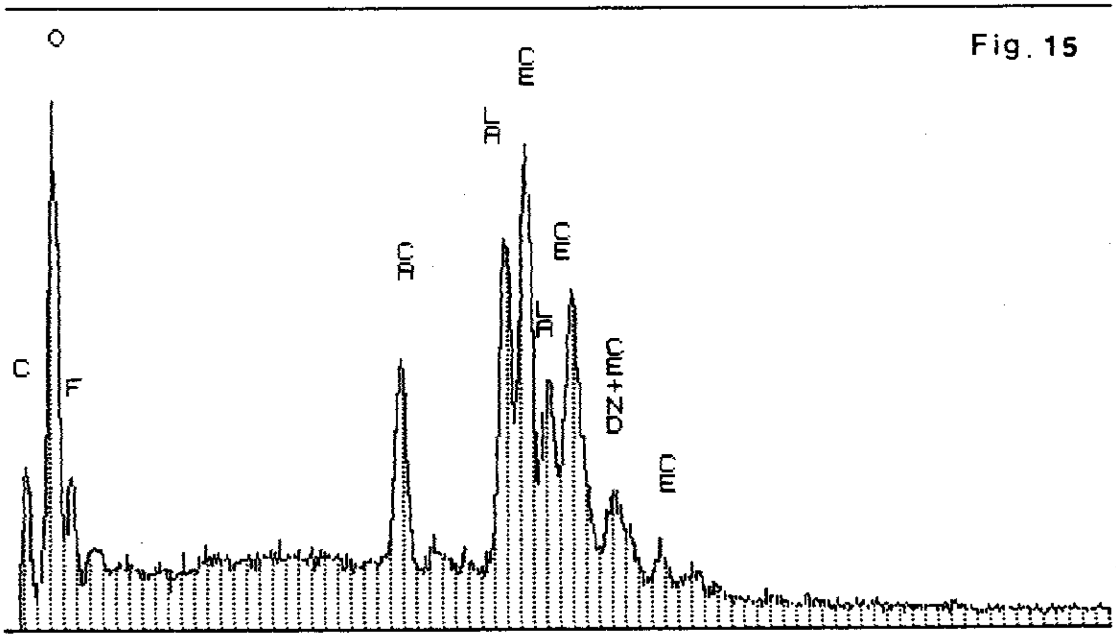

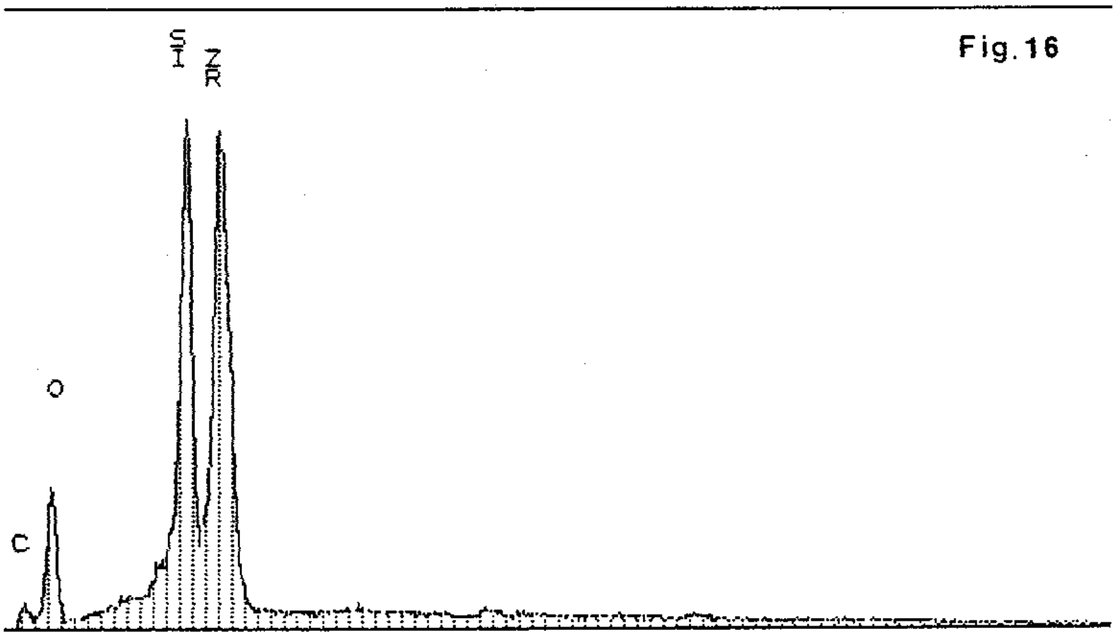

Fig. 15 EDS spectra of parisite.

Fig. 16 EDS spectra of zircon.

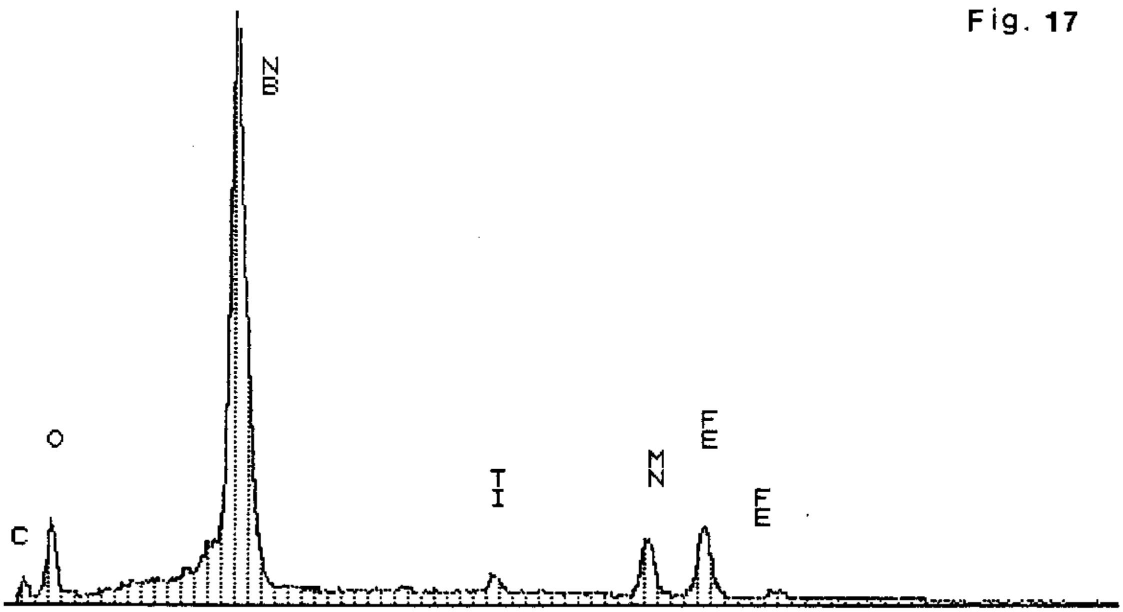

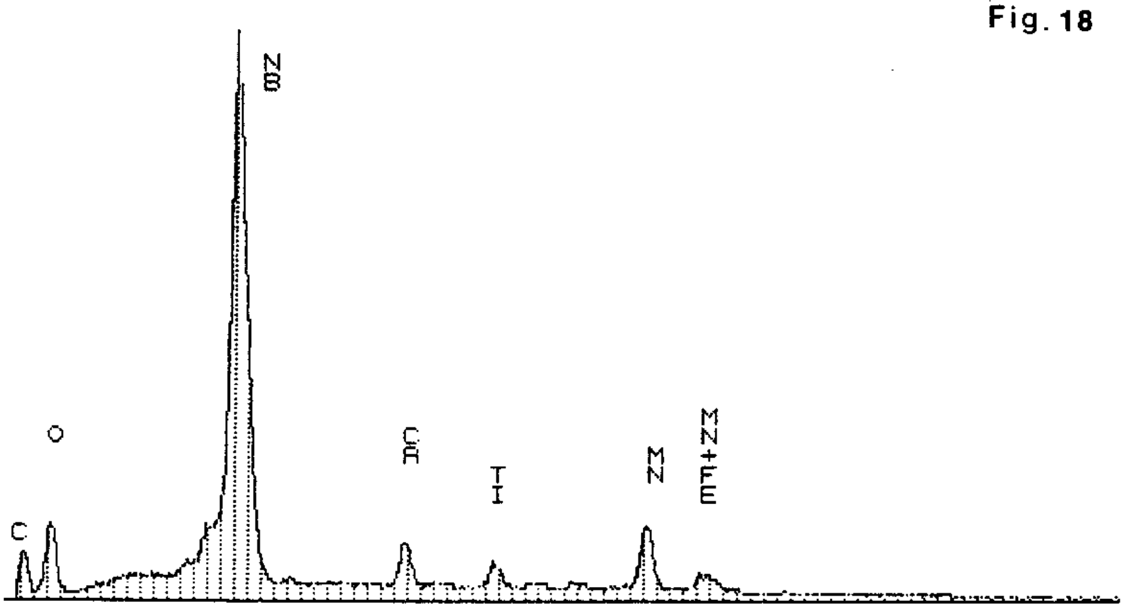

Fig. 17 EDS spectra of ferrocolumbite.

Fig. 18 EDS spectra of manganocolumbite.

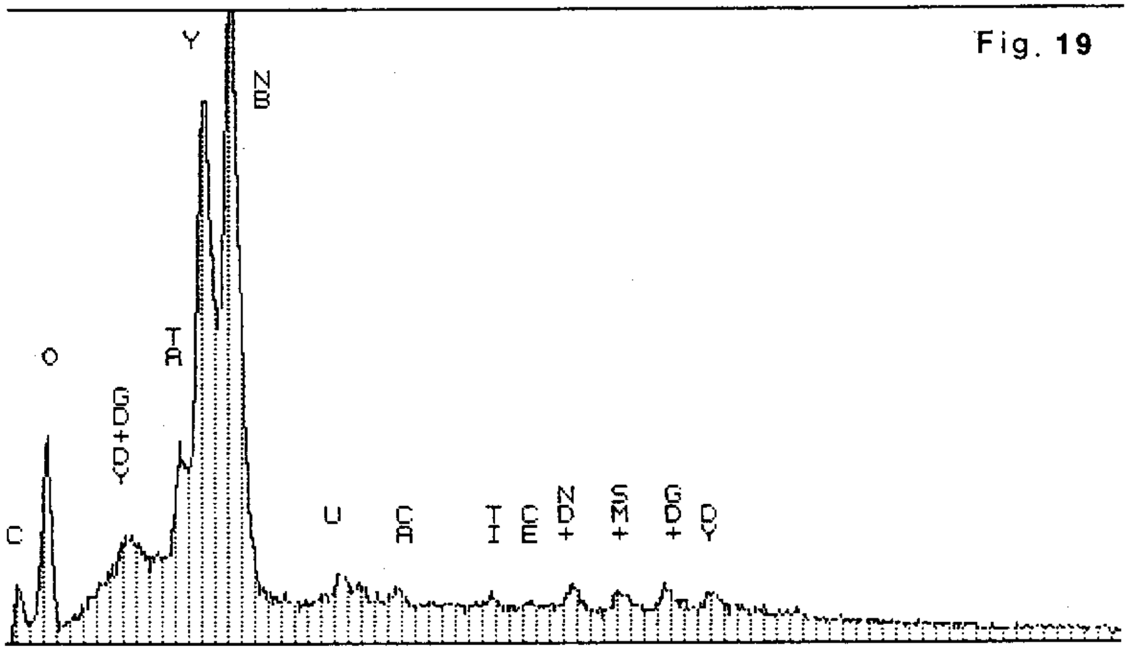

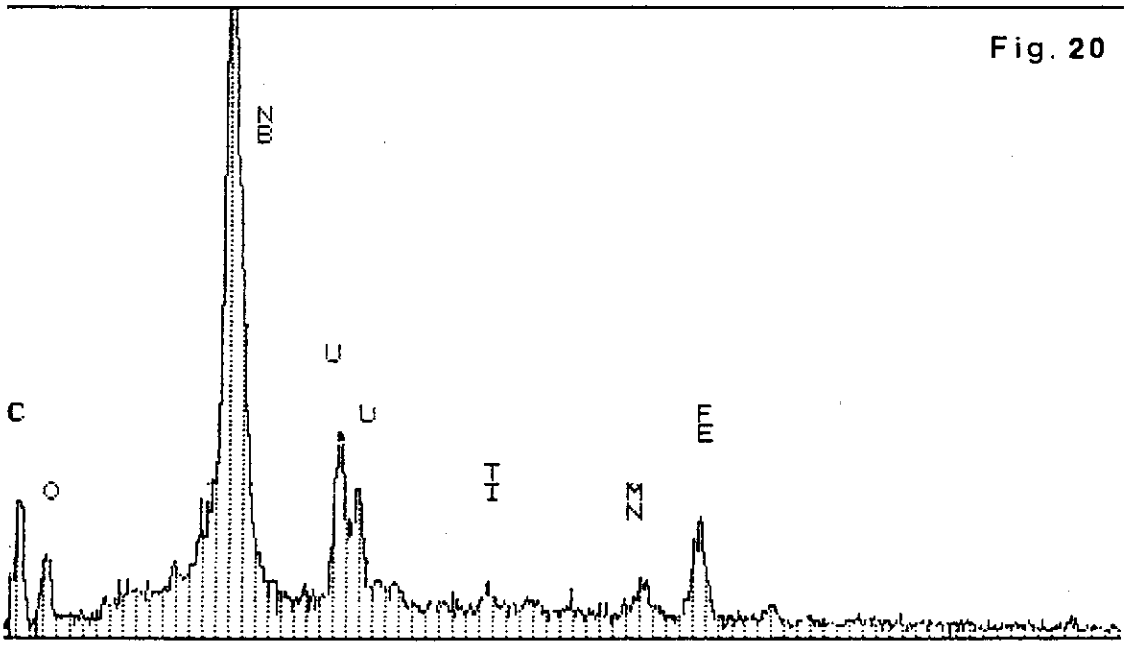

Fig. 19 EDS spectra of yttrocolumbite.

Fig. 20 EDS spectra of uranium-bearing niobate.

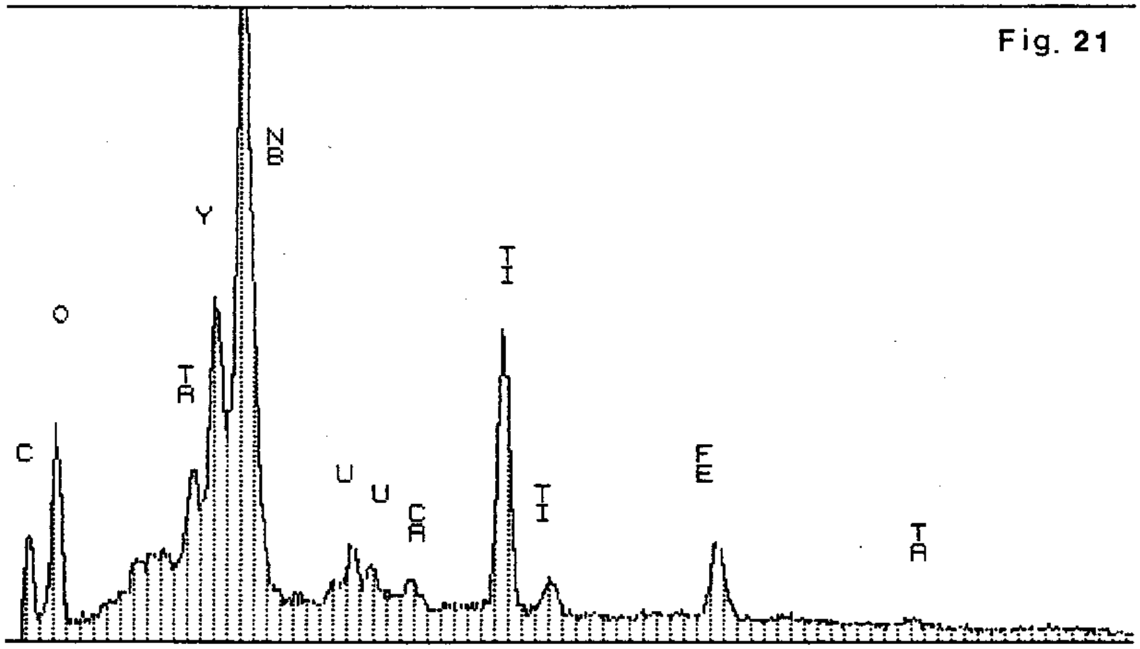

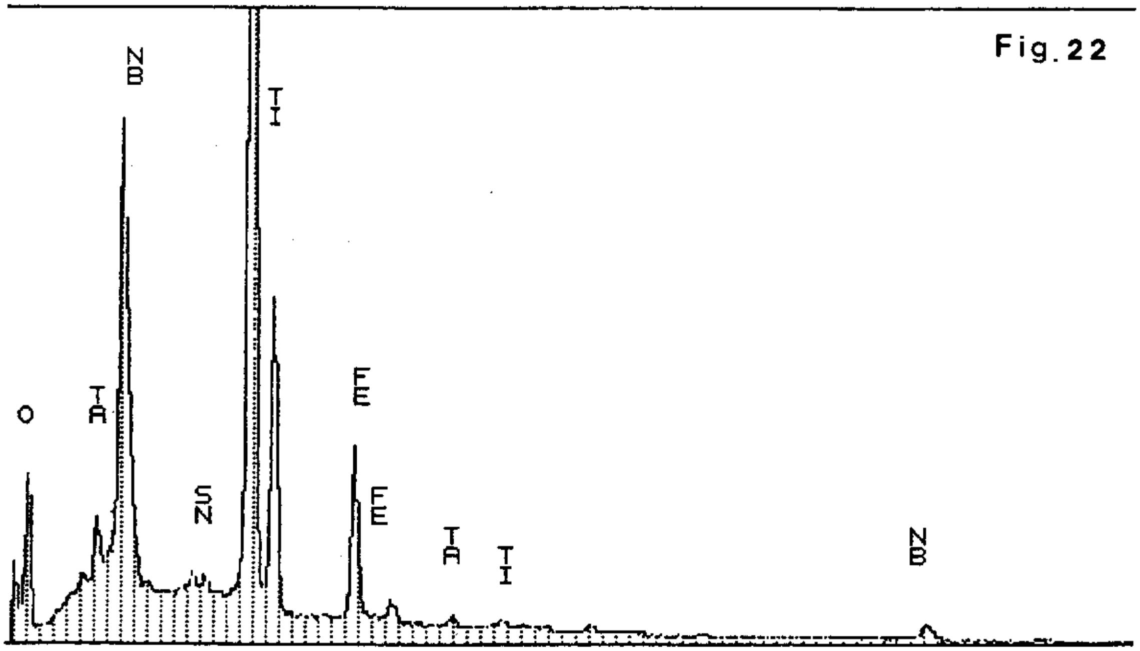

Fig. 21 EDS spectra of yttrobetafite?

Fig. 22 EDS spectra of aeschynite?

Fig. 23

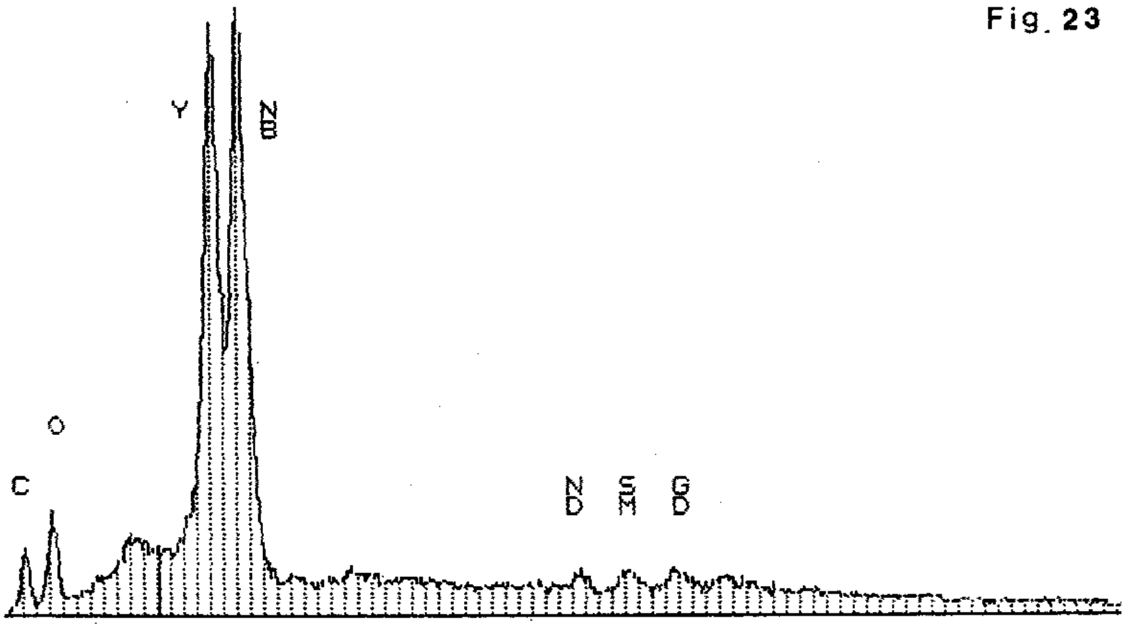

Fig. 24

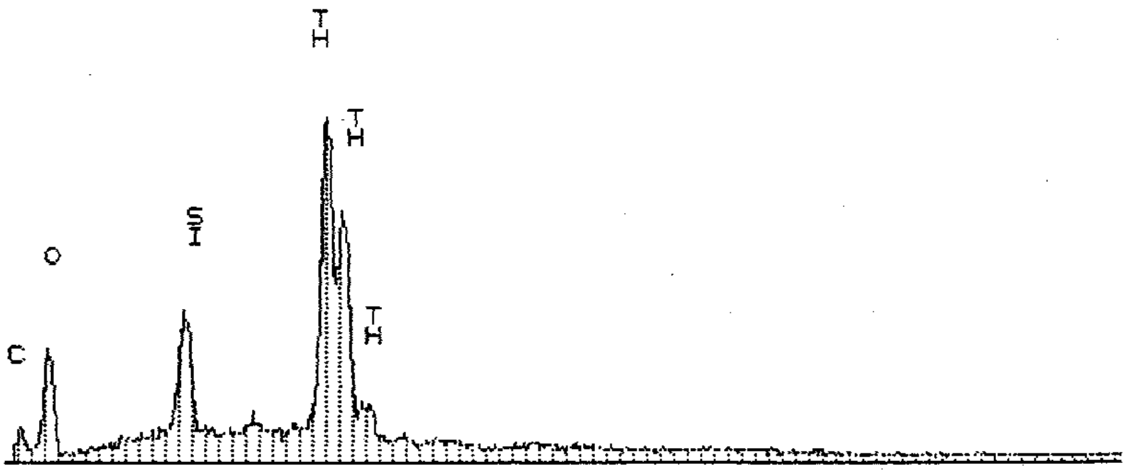

Fig. 23 EDS spectra of fergusonite-(Y).

Fig. 24 EDS spectra of thorium silicate.

MINERALOGICAL ANALYSIS OF ORE SPECIMENS FROM THE RARE EARTH DEPOSIT OF DODGEX LTD.

PART II
QUANTITIES OF RARE EARTH MINERALS AND THEIR LIBERATION CHARACTERISTICS

SEPTEMBER 1995

MINERAL SCIENCES LABORATORIES
R. Lastra and D. Owens

Work performed for:
J.S. Dodge
Dodgex Ltd.
Whitehorse, Yukon

Job No. 51075

CONFIDENTIAL

MINERAL SCIENCES LABORATORIES
DIVISION REPORT MSL 95-43 (CR)

CANMET

EXECUTIVE SUMMARY

A mineralogical study was conducted on rare earth-bearing samples from the Lancer deposit in Yukon, at Dodgex Ltd. Two samples, labelled "mainvein" and "footwall" were analysed. The purpose of the study is to provide guidance for designing processing tests aimed at concentrating the rare earth minerals.

It was found that the mainvein ore contains 8636 ppm Zr, 4089 ppm Nb, 1049 ppm Y, 6297 ppm Ce, 3903 ppm La, and 1886 ppm Nd. The footwall ore contains 9380 ppm Zr, 6888 ppm Nb, 1094 ppm Y, 6520 ppm Ce, 3695 ppm La, and 1997 ppm Nd. The samples also contain small quantities of Pr, Sm, Gd, and Dy, and trace amounts of Eu, Tb, Ho, Er, Tm, Yb and Lu.

The main rare earth mineral is monazite ($(Ce,La,Nd,Th)PO_4$). For the mainvein ore, a grind to 80% -170 mesh (80% -250 mesh for footwall ore) will liberate 50 to 60% of the monazite, whereas a grind to 80% -250 mesh (80% -400 mesh for footwall ore) will liberate 65 to 75% of the monazite.

The second major rare earth mineral is bastnaesite ($(Ce,La)(CO_3)F$). For the mainvein ore, a grind to 80% -250 mesh (80% -270 mesh for footwall ore) will liberate 50 to 60% of the bastnaesite, whereas a grind to 80% -325 mesh (80% -400 mesh for footwall ore) will liberate 65 to 75% of the bastnaesite.

The Zr occurs as the major constituent of a poorly-crystallized spongy zircon ($ZrSiO_4$). The zircon is present as minute inclusions in silicates, bastnaesite/parisite and columbite. For the mainvein ore a grind to 80% -800 mesh (80% -1400 mesh for footwall ore) will liberate 65 to 75% of the zircon.

The Nb occurs as the major constituent of a variety of minerals grouped under the generic term "niobates," with ferrocolumbite ($Fe^{+2}Nb_2O_6$) and manganocolumbite ($Mn^{+2}Nb_2O_6$) being the main niobium minerals. For the mainvein ore a grind to 80%

-325 mesh (80% -500 mesh for footwall ore) will liberate 65 to 75% of the ferrocolumbite. For the mainvein ore a grind to 80% -270 mesh (80% -500 mesh for footwall ore) will liberate 65 to 75% of the manganocolumbite.

The required grinds to liberate the rare earth minerals are finer for the footwall ore than for the mainvein ore. This is due to the smaller mineral grain sizes found in the footwall ore. Relatively coarser grinds are required to liberate monazite and bastnaesite which are the major rare earth minerals. However, the required grinds to liberate most of the other rare earth minerals are very fine and un-practical for effective mineral processing. Therefore, it is recommended to design the mineral processing tests to concentrate monazite and bastnaesite and accept whatever recovery is obtained for the other less abundant, rare earth minerals. Fifty to sixty percent of the monazite in the mainvein ore would be in particles with at least 70% of monazite by grinding the ore to 80% -170 mesh. At this grind a pre-concentration operation could be performed. Then a re-grind to 80% -400 mesh could be performed followed by other concentration steps. Also leaching tests on the un-ground and re-grinded pre-concentrate should be considered.

It is suggested that gravity separation devices be considered for pre-concentration tests of the ore ground to 80% -170 mesh (80% -90 μm). Many gravity separation devices do not successfully treat material in the 100 μm range. However, devices like the shaking table and the Bartles-Mozley table have been used to effectively treat material in the 100 μm range. It is also suggested that the mainvein ore be treated separately from the footwall ore in the mineral processing tests, at least in the pre-concentration step.

Keywords: rare earth minerals, monazite, bastnaesite, estimation of liberation grinds

CONTENTS

INTRODUCTION

A mineralogical and image analysis study of rare earth-bearing samples from the Lancer deposit in Yukon was undertaken by the Applied Mineralogy Group as a cost recovery project. The deposit is owned by Dodgex Limited, and a MDA grant was contributed by the Yukon Department of Natural Resources for a mineralogical characterization which would provide guidance in processing the ore. A contract was drawn-up between CANMET (CANMET/MSL Project 51075) and Mr. Dodge, President, Dodgex Ltd., 14 MacDonald Road, Whitehorse, Yukon on February 3, 1995. Two 100 kilogram samples of the ore were received by CANMET on February 17, 1995 from Mr. Dodge. The samples consisted of rock fragments averaging ≈30 cm in size, and were labelled "mainvein" and "footwall".

The mineralogical and image analysis study was performed in two parts. The first part, to identify the rare earth minerals and to determine their compositions and mode of occurrence has already been submitted to Dodgex Ltd. This report is Part II and deals with the relative quantities of rare earth minerals and their liberation characteristics.

METHOD OF INVESTIGATION

The same sample preparation procedure was followed for Part I and for Part II of the investigation. The rock fragments from the two samples were crushed to -4.7 mm (-4 mesh) and split into 50 kg subsamples. One sub-sample of each type was crushed to -1.7 mm (-10 mesh). A 2 kg sample was then split from the "mainvein" and "footwall" sub-samples and ground to -295 μm (-48 mesh). Size fractionation was performed on the -48 mesh product and, in addition, the -147+45 μm (-100+325 mesh) fractions were separated into sink and float sub-fractions using a heavy liquid with a specific gravity of 3.30. The two sink fractions, in which the rare earth ore minerals were concentrated were mounted in polished sections. This procedure already suggests that the rare earth minerals are amenable to gravity concentration.

The polished sections were studied with a KONTRON-IBAS image analyser coupled with a JEOL -733 electron microprobe and an energy dispersive system. An image analysis program of more than 1200 lines was specifically developed for this part of the study. The program was designed in basis of the general mineralogy findings given in PART I of the report (Lastra and Owens, April 1995). The image analysis was executed using backscattered electron (BSE) images to discriminate the gangue minerals (quartz, albite, pyroxene, muscovite, ankerite, dolomite, siderite, calcite and rhodochrosite), the iron oxides (goethite and magnetite), pyrite, and zircon. The rare earth minerals were segmented into three image-groups at the higher end of the BSE grey level. These groups included, chalcopyrite, sphalerite and metallic iron (contamination from grinding). The discrimination between the minerals in the rare-earth groups was done by an energy dispersive scan on each mineral grain to determine the X-ray counts for sixteen elements: La, Ce, P, Ca, Si, Y, Zr, Nb, U, Fe, Mn, Ti, Th, Cu, Zn and S. The X-ray counts for each mineral grain were normalized and used in a classification algorithm to discriminate between the minerals in the three groups. The following rare earth minerals were thus discriminated: monazite, bastnaesite, parisite, ferrocolumbite, manganocolumbite, uranium-niobate, fergusonite-(Y), yttrocolumbite, yttrobetafite, aeschynite, thorite, and zircon. Chalcopyrite, sphalerite and metallic iron were left in one group, since discrimination between these minerals is not important for the present study. A meander of 10x10 contiguous frames was done at a magnification of 100 times. Therefore a total of one hundred BSE images was analysed. The image analysis program written for this job was set up to determine the mineral quantities and to measure the grain size distribution of each of the discriminated rare earth minerals to estimate their liberation grinds. Approximately 4000 particles were analysed in the meander for each polished section.

RESULTS

SAMPLE FRACTIONATION

Data for the size fractionation performed on the ground samples to -48 mesh are given in Table 1. Size fractions -100+200 and -200+325 were joined to form the

-100+325 mesh fraction which was separated into sink and float sub-fractions using a heavy liquid with a specific gravity of 3.30. Table 2 gives the proportions of sink and float products. Approximately 2.7 wt% of the -100+325 mesh fraction reports to the heavy mineral concentrate.

RELATIVE MINERAL QUANTITIES

The mineral quantities measured by image analysis in the heavy mineral concentrate fraction are given in Table 3. It should be noted that yttrobetafite was reported in Part I to contain Nb, Y, Ti, Ta, and Fe. At the time of setting the image analysis program it was found that yttrobetafite also contained Rb, U, and Th.

Table 3 shows that monazite is the most abundant rare earth mineral, followed by bastnaesite, ferrocolumbite and zircon. The microprobe analysis of the rare earth minerals (Part I) reported no significant difference between them in the mainvein sample and in the footwall sample, the chemical assays also showed that the two samples are similar and the quantity of heavy mineral concentrate from both samples is similar. Table 3 shows that the mainvein ore is apparently richer in rare earth minerals than the footwall ore. The heavy mineral concentrate from the mainvein has 25 wt% monazite whereas the concentrate from the footwall has ≈ 10 wt% monazite. However, the higher concentration of rare earth minerals in the concentrate of the mainvein is due to a higher liberation of these minerals in the -100+325 size fraction of the mainvein ore.

Polished sections prepared from the un-concentrated -48+65 size fraction were also studied with a scanning electron microscope. However, it was very difficult to locate rare earth mineral grains. Therefore the strategy of using a heavy liquid to produce a heavy mineral concentrate proved very useful in the characterization of the rare earth minerals. Table 3 also gives an estimate of the quantity of rare earth mineral in the original un-concentrated sample. This estimate was calculated from the amount of heavy mineral concentrate and the measured quantities of rare earth minerals in it. The estimated quantities of rare earth mineral in the original samples are not accurate, and are solely given to provide order of magnitude amounts. These very low amounts prevent reliable determination of the quantities directly from polished sections of the original un-concentrated samples. Therefore chemical assays for the rare earth elements in the original samples (Table 1 in Part I) should be used to estimate the reserves of the ore.

ESTIMATED LIBERATION GRIND

As described in Part I, the grain size of the rare earth minerals is quite fine. Due to this fact, it is possible to estimate the required grinds for liberation from grain size measurements in the heavy mineral concentrate from the -100+325 size fraction. This fraction still preserves the grain size distribution found in the un-ground ore. The heavy mineral concentrates also provide a large grain population of the major rare earth minerals thus allowing a better estimation of the required grind for liberation. The measured populations for monazite, bastnaesite, zircon and ferrocolumbite was approximately 3,300, 2,500 1,500 and 1,000 grains respectively. Thus, the estimated liberation for these minerals is more reliable.

The results of the measured grain size are plotted to give the cumulative grain size distribution (Figures 1 to 6). The X-axis of these figures gives the size (μm) of the mineral grains; the Y-axis gives the cumulative weight percent of the mineral in grains finer than the given size. For example, Fig. 1 shows that 70% of the monazite in the heavy mineral concentrate of the mainvein sample is finer grained than 75 μm (=200 mesh).

Figure 1 gives the cumulative grain size distribution, in the mainvein sample, for monazite (mona), bastnaesite (basn), zircon (zir), and ferrocolumbite (Fe-cmb). Figure 2 gives the cumulative grain size distribution for parisite (paris), yttrobetafite (Y-beta), uranium niobate (U-nb) and yttrocolumbite (Y-cmb). The grain size distribution curves for parisite and uranium niobate are average trends. This was done because of the small number of parisiste and uranium-niobate grains in the sample. The average for each point was calculated from the measured data at the point and the measured data at the two adjacent points. Figure 3 gives the cumulative grain size distribution for manganocolumbite (Mn-cmb), thorite (thor), aeschynite (aschy), and fergusonite-(Y) (Y-ferg). Again, curves for manganocolumbite and aeschynite are average trends. Similarly, Figures 4 to 6 give the grain size distributions in the footwall sample.

These figures can be used to estimate the required grinds to achieve liberation of the minerals. According to Petruk (1986), the grain size distribution of a mineral is the basis for predicting a minimum, an optimum and a practical grind for liberating the mineral.

Minimum grind is considered to be equal to the size distribution of the mineral in the unbroken ore. When the ore is ground to this size, liberation of the mineral is expected to be around 50 to 60%. That is, 50 to 60% of the mineral in the ore will be in particles with at least 70% of that mineral.

Optimum grind is defined as the size below which liberation does not improve significantly. This occurs when there is a significant change of slope going from finer sizes to coarser sizes. In practice there is a compromise between the values for minimum grind and optimum grind. Such grind is referred to as the practical grind.

The minimum grind is indicated in Figures 1 to 6 by the arrow at 80% in the Y-axis, the practical grind is indicated by an arrow at 50%. The estimated minimum grind, practical grind, and the optimum grind obtained from Figures 1 to 6 are summarised in Tables 4 and 5. Table 4 gives the grind sizes in micrometres and Table 5 in "mesh" units. The data in brackets are for the "footwall" sample, those not in brackets are for the "mainvein" sample. The predicted liberation in the tables is given considering the percentage of the mineral of interest that would be in particles with at least 70% of that mineral.

RECOMMENDATIONS

The data in Table 4 (or Table 5) shows that the footwall ore needs to be ground finer than the mainvein ore to achieve a given liberation. This is due to the smaller mineral grain sizes found in the footwall ore. Relatively coarser grinds are required to liberate monazite and bastnaesite, which are the major rare earth minerals. However, very fine grinds are required to liberate most of the other rare earth minerals. Therefore it is recommended that the mineral processing tests be designed to concentrate the monazite and the bastnaesite and accept whatever recovery is achieved of the other, less abundant rare earth minerals. Table 5 shows that 50 to 60% of monazite in the mainvein ore would be in particles with at least 70% of monazite by grinding the ore to 80% -170 mesh. At this grind a pre-concentration operation could be performed. Then re-grind to 80% -400 mesh and perform other concentration steps. Even though a grind to 80% -500 is too fine for many mineral processing concentration operations, some re-grind tests to that point should be considered, because the liberation data indicates a high liberation for monazite at that grind. Also leaching tests on the un-ground and re-grinded pre-concentrate should be considered.

It is also suggested that gravity separation devices be considered for pre-concentration tests of the ore ground to 80% -170 mesh (80% -90 μm). Many gravity separation devices do not successfully treat material in the 100 μm range. However, devices like the shaking table and the Bartles-Mozley table have been used to treat effectively material in the 100 μm range.

ACKNOWLEDGEMENTS

The authors would like to thank J.M. Beaulne for preparation of the polished sections and for size and heavy liquid separations.

REFERENCES

R. Lastra and D. Owens, (April 1995), Mineralogical analysis of ore specimens from the rare earth deposit of Dodgex Ltd. Part I: Mineral identities, compositions and modes of occurrence. CANMET, Mineral Sciences Laboratories, Division Report MSL 95-25(CR).

W. Petruk, (1986), Predicting and measuring mineral liberation in ores and mill products, and effect of mineral textures and grinding methods on mineral liberations. Process Mineralogy VI, Ed. R.D. Hagni, AIME/SME, Warrendale, PA, pp. 393-403.

Table 1 - Size fractionation of the -48 mesh ground samples

Size fraction		Weight %	
[μm]	[mesh]	mainvein	footwall
-295+208	-48+65	15.7	18.6
-208+147	-65+100	12.6	12.1
-147+74	-100+200	23.6	19.8
-74+45	-200+325	14.9	14.1
-45	-325	33.2	35.5

Table 2 - Heavy mineral concentration using a liquid with a specific gravity of 3.3

PRODUCT	Weight %	
	mainvein	footwall
Float	97.1	97.4
Sink	2.9	2.6

Table 3 - Mineral quantities as determined by image analysis in the heavy mineral concentrate of samples from "mainvein" and "footwall"

MINERAL OR MINERAL GROUP	QUANTITY OF MINERAL wt % MAINVEIN Heavy mineral concentrate	MAINVEIN Original sample (estimated)	FOOTWALL Heavy mineral concentrate	FOOTWALL Original sample (estimated)
gangue	29.8		57.5	
iron oxides	10.3		3.26	
pyrite	22.5		15.7	
zircon	1.2	0.03	1.3	0.03
ferrocolumbite	3.3	0.1	1.8	0.05
manganocolumbite	0.1	0.003	1.6	0.04
uranium niobate	0.02	0.0006	0.05	0.001
fergusonite-(Y)	0.002	0.00006	0.0004	0.00001
yttrocolumbite	0.2	0.006	0.02	0.0005
yttrobetafite	0.2	0.006	0.1	0.003
aeschynite	0.004	0.0001	0.005	0.0001
monazite	25.2	0.7	9.7	0.2
parisite	0.3	0.01	0.4	0.01
bastnaesite	6.9	0.2	8.5	0.22
thorite	0.03	0.001	0.002	0.00005
chalcopyrite, sphalerite and metallic iron	0.04		0.05	

Table 4 - Estimated minimum, practical and optimum grind for liberation, all values in micrometres. Data inside brackets are for the minerals in the "footwall" sample, those not in brackets are for the minerals in the "mainvein" sample.

	Minimum grind, 80% passing (predicted liberation 50 to 60%)	Practical grind, 80% passing (predicted liberation 65 to 75%)	Optimum grind, 80% passing (predicted liberation 85 to 95%)
monazite	90 (63) μm	63 (37) μm	26 (13) μm
bastnaesite	63 (52) μm	45 (37) μm	18 (13) μm
ferrocolumbite	63 (37) μm	45 (≈26) μm	18 (9.4) μm
zircon	≈37 (≈26) μm	≈18 (≈13) μm	9.4 (6.6) μm
parisite	147 (45) μm	52 (18) μm	13 (6.6) μm
yttrobetafite	≈26 (26) μm	≈18 (18) μm	9.4 (6.6) μm
uranium niobate	90 (45) μm	52 (26) μm	9.4 (9.4) μm
yttrocolumbite	74 (18) μm	45 (13) μm	18 (4.6) μm
manganocolumbite	90 (45) μm	52 (26) μm	9.4 (9.4) μm
thorite	≈26 (4.6) μm	≈18 (3.3) μm	9.4 (≤3.3) μm
aeschynite	≈37 (≈18) μm	≈18 (≈9.4) μm	6.6 (4.6) μm
fergusonite-(Y)	≈9.4 (≤4.6) μm	6.6 (3.3) μm	4.6 (≤3.3) μm

Table 5 - Estimated minimum, practical and optimum grind for liberation, all values in mesh units. Data inside brackets are for the minerals in the "footwall" sample, those not in brackets are for the minerals in the "mainvein" sample.

	Minimum grind, 80% passing (predicted liberation 50 to 60%)	Practical grind, 80% passing (predicted liberation 65 to 75%)	Optimum grind, 80% passing (predicted liberation 85 to 95%)
monazite	170 (250) mesh	250 (400) mesh	500 (1400) mesh
bastnaesite	250 (270) mesh	325 (400) mesh	800 (1400) mesh
ferrocolumbite	250 (400) mesh	325 (≈500) mesh	800 (1600) mesh
zircon	≈400 (≈500) mesh	≈800 (≈1400) mesh	1600 (2400) mesh
parisite	100 (325) mesh	270 (800) mesh	1400 (2400) mesh
yttrobetafite	500 (500) mesh	≈800 (800) mesh	1600 (2400) mesh
uranium niobate	170 (325) mesh	270 (500) mesh	1600 (1600) mesh
yttrocolumbite	200 (800) mesh	325 (1400) mesh	800 (3200) mesh
manganocolumbite	170 (325) mesh	270 (500) mesh	1600 (1600) mesh
thorite	≈500 (3200) mesh	≈800 (≤3200) mesh	1600 (≤3200) mesh
aeschynite	≈400 (≈800) mesh	≈800 (≈1600) mesh	2400 (3200) mesh
fergusonite-(Y)	≈1600 (≤3200) mesh	2400 (≤3200) mesh	3200 (≤3200) mesh

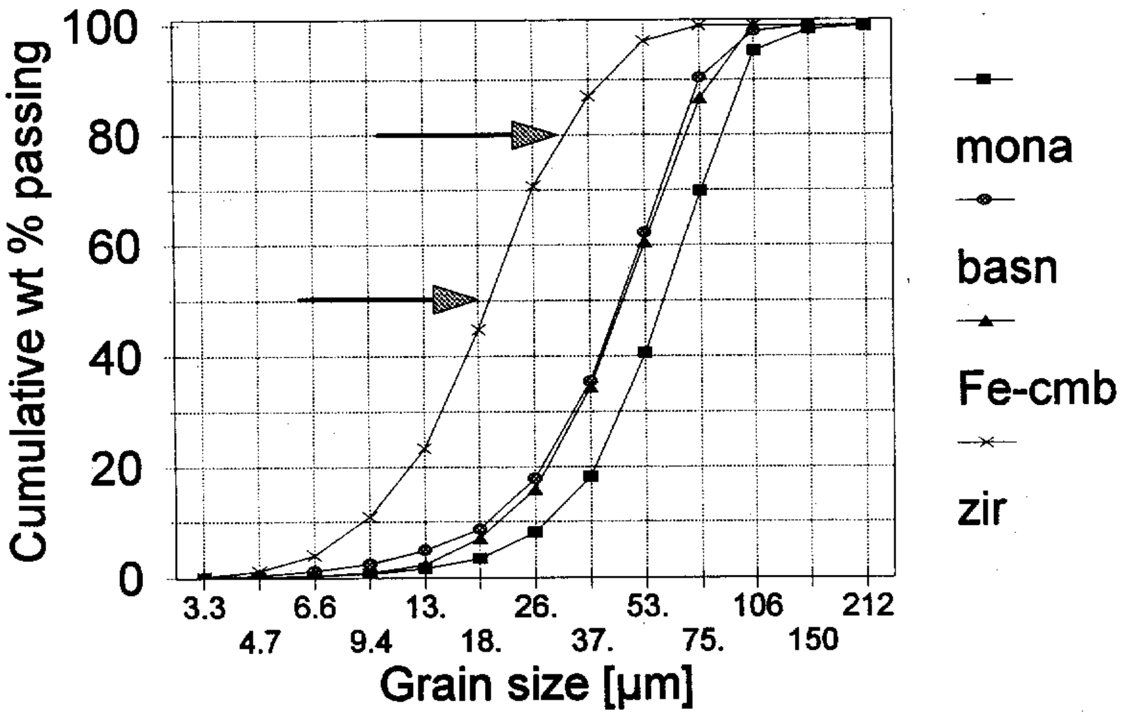

Fig. 1 - Cumulative grain size distribution for monazite (mona), bastnaesite (basn), zircon (zir), and ferrocolumbite (Fe-cmb) in the mainvein ore.

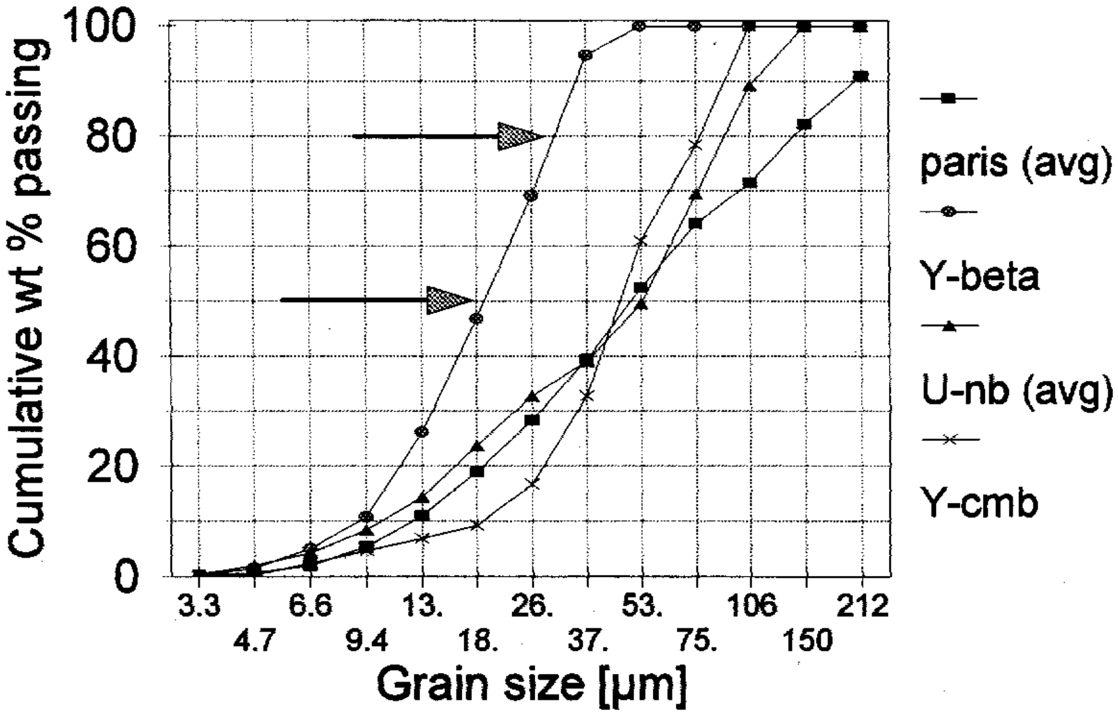

Fig. 2 - Cumulative grain size distribution for parisite (paris), yttrobetafite (Y-beta), uranium niobate (U-nb) and Yttrocolumbite (Y-cmb) in the mainvein ore. The grain size distribution curves for parisite and uranium niobate are average trends.

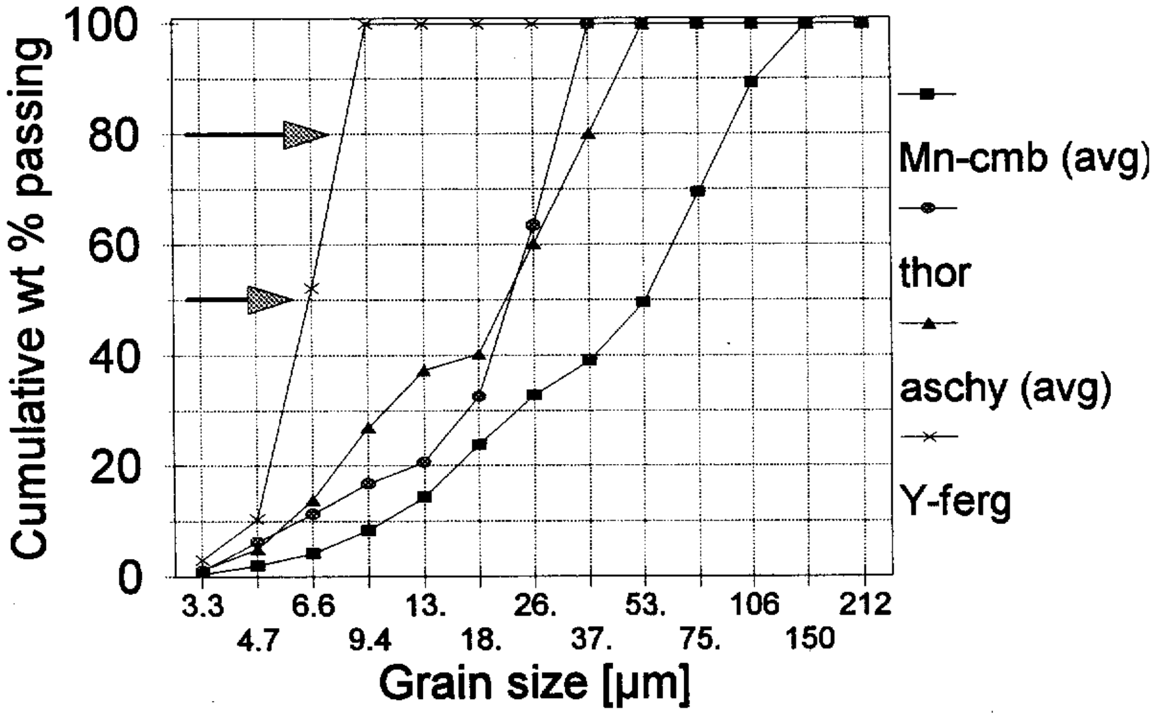

Fig. 3 - Cumulative grain size distribution for manganocolumbite (Mn-cmb), thorite (thor), aeschynite (aschy), and fergusonite-(Y) (Y-ferg) in the **mainvein ore**. Curves for manganocolumbite and aeschynite are average trends.

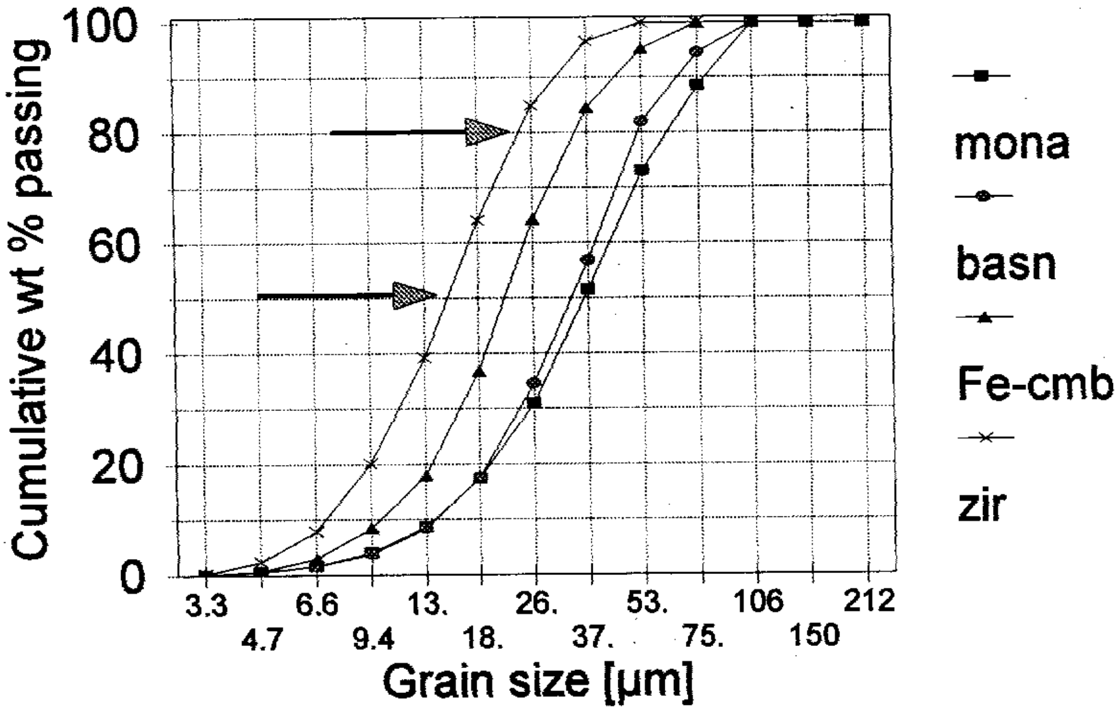

Fig. 4 - Cumulative grain size distribution for monazite (mona), bastnaesite (basn), zircon (zir), and ferrocolumbite (Fe-cmb) in the **footwall ore**.

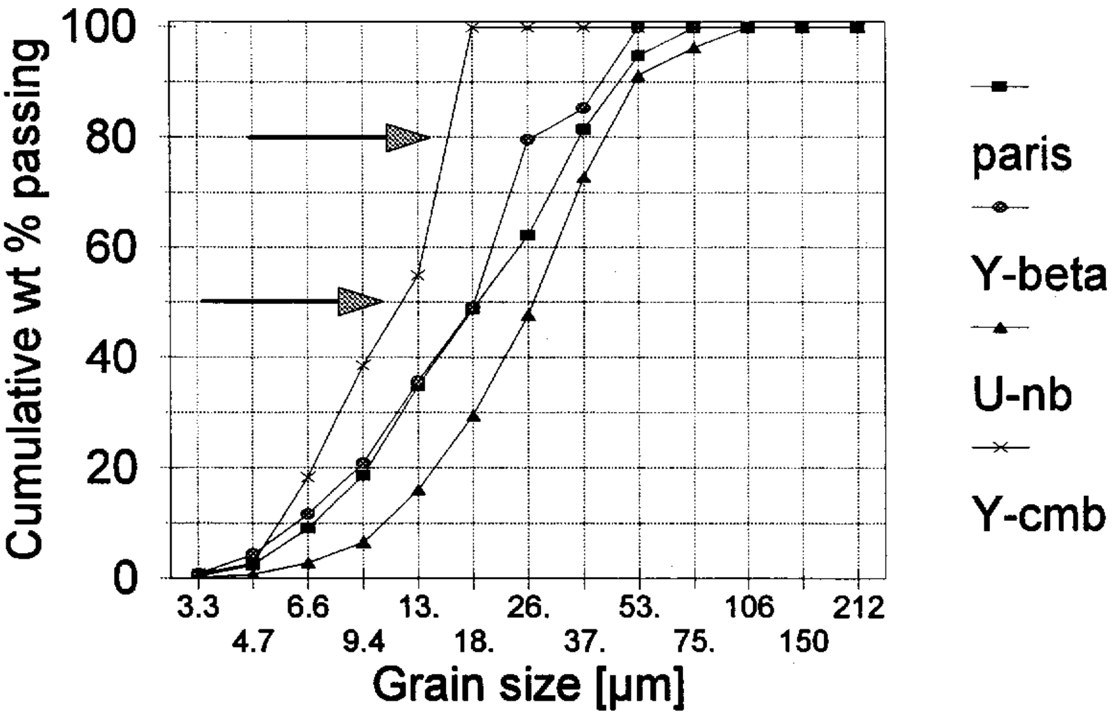

Fig. 5 - Cumulative grain size distribution for parisite (paris), yttrobetafite (Y-beta), uranium niobate (U-nb) and Yttrocolumbite (Y-cmb) in the footwall ore.

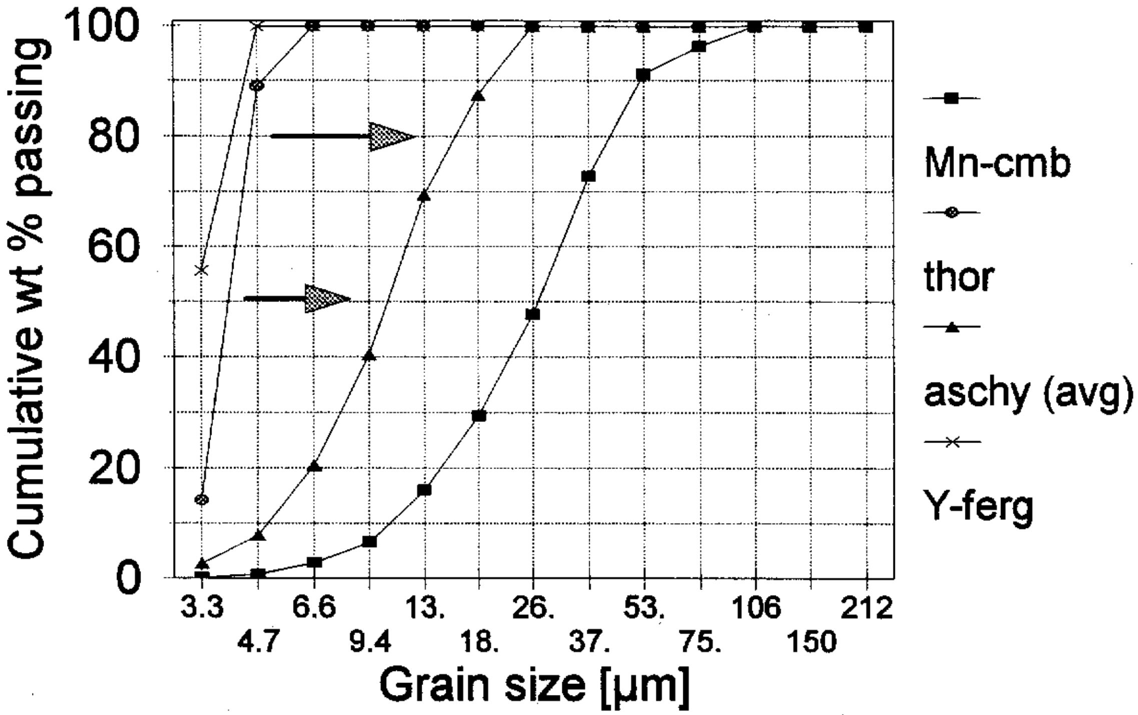

Fig. 6 - **Cumulative grain size distribution for manganocolumbite (Mn-cmb), thorite (thor), aeschynite (aschy), and fergusonite-(Y) (Y-ferg) in the footwall ore.** Curve for aeschynite is an average trend.